Article

Journal of
Nanoscience and Nanotechnology
Vol. 15, 8176–8182, 2015
www.aspbs.com/jnn

Roughening of Polyimide Surface for Inkjet Printing by Plasma Etching Using the Polyimide Masked with Polystyrene Nanosphere Array

Mu Kyeom Mun[1], Jin Woo Park[1], Jin Ho Ahn[3], Ki Kang Kim[3], and Geun Young Yeom[1, 2, *]

[1] *Department of Materials Science and Engineering, Sungkyunkwan University, Suwon, Gyeonggi-do, 440-746, South Korea*
[2] *SKKU Advanced Institute of Nanotechnology (SAINT), Sungkyunkwan University, Suwon, Gyeonggi-do 440-746, South Korea*
[3] *Department of Materials Science and Engineering, Hanyang University, Seoul, 133-791, South Korea*

Two key conditions are required for the application of fine-line inkjet printing onto a flexible substrate such as polyimide (PI): linewidth control during the inkjetting process, and a strong adhesion of the polyimide surface to the ink after the ink solidifies. In this study, the properties of a polyimide surface that was roughened through etching in a He/SF_6 plasma, using a polystyrene nanosphere array as the etch mask, were investigated. The near-atmospheric-pressure plasma system of the He/SF_6 plasma that was used exhibits two notable properties in this context: similar to an atmospheric-pressure plasma system, it can easily handle inline substrate processing; and, similar to a vacuum system, it can control the process gas environment. Through the use of plasma etching, the polyimide surface masked the 120-nm-diameter polystyrene nanospheres, thereby forming a roughened nanoscale polyimide surface. This surface exhibited not only a greater hydrophobicity—with a contact angle of about 150° for water and about 30° for silver ink, indicating better silver linewidth control during the silver inkjetting process—but also a stronger adhesion to the silver ink sprayed onto it when compared with the flat polyimide surface.

Keywords: Polystyrene Nanosphere, Near-Atmospheric-Pressure Plasma, Surface Roughening, Polyimide, Ink Jet.

1. INTRODUCTION

Flexible electronic devices are widely researched, as they are the next generation of devices for technologies including displays and photovoltaics (PV). Polymer substrates such as polyimide (PI), polyethylene naphthalate (PEN), and polyethylene terephthalate (PET) are widely used as the substrates for these flexible devices. To form a device structure on the polymer substrates, fine-line patterns for microelectronics are required, and these patterns can generally be formed by conventional integrated circuit (IC) fabrication techniques including lithography, thin film deposition, and etching;[1, 2] however, conventional IC fabrication techniques require expensive vacuum processing equipment and it is difficult to increase the size of the substrate.[3]

As an alternative to IC fabrication techniques, direct printing techniques such as microcontact printing, nano imprinting, screen printing, and inkjet printing[4–11] have been investigated. Among these techniques, difficulties have been observed in microcontact printing and nano imprinting, among others, regarding large-sized printing areas. Screen printing requires high levels of ink consumption and difficulties arise in the production of fine-line patterns.[12] In the case of inkjet printing, a lesser amount of expensive ink is needed and the technique is performed without substrate contact, meaning that the substrate is not physically damaged during the inkjetting process.[13] In the current time period, the utility of inkjet printing technology in the flexible electronics field has been researched more intensively, due not only to its high throughput and low cost, but also because it is capable of producing fine metal lines on polymer substrates.

*Author to whom correspondence should be addressed.

1533-4880/2015/15/8176/007 doi:10.1166/jnn.2015.11285

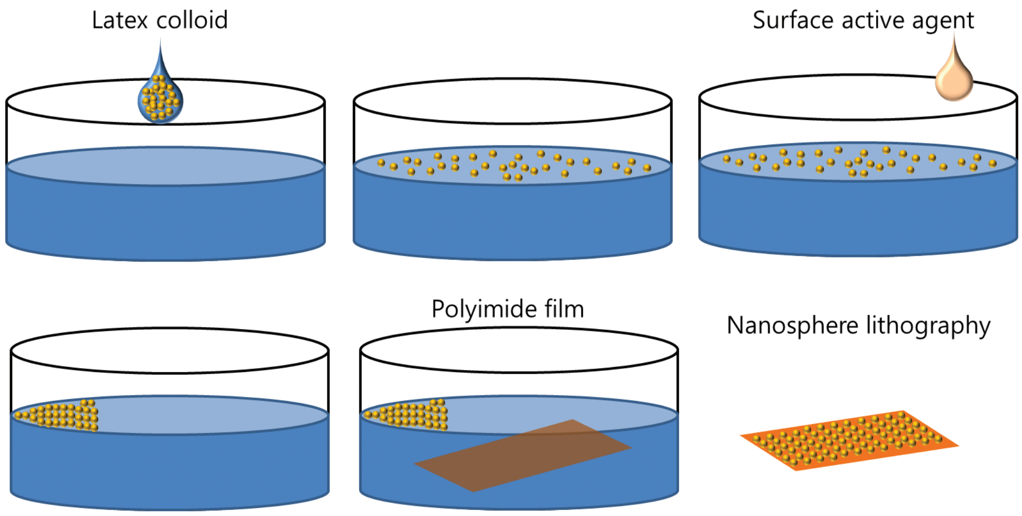

Figure 1. The nanosphere lithographic (NSL) process used in the experiment to mask the PI surface with the polystyrene nanosphere array. Polystyrene nanospheres (polystyrene collioid) with a 120 nm diameter were used.

Despite the above-mentioned advantages, to apply the inkjet-printing technique for the production of next-generation flexible electronic devices, greater fine-linewidth control and a stronger adhesion of the inkjet-printed metal lines to the substrate are required.[14,15] To control the linewidth, numerous methods have been investigated including inkjet-module quality enhancement and substrate temperature control;[16–20] however, these methods do not enhance the adhesive qualities of the lines. To enhance the adhesion of the lines to the substrate, techniques such as adhesive use and surface treatment have been explored, but it is difficult to control the linewidth with such methods.[21,22] Recently, the texturing of the polymer surface to produce a microroughness resulted in an enhancement of both linewidth control and the adhesion to the substrate, whereby PI, which is greatly advantageous because it is thermally and chemically stable, was used as the substrate.[23] In this method, to obtain a microroughened PI surface, a thin, porous oxide layer was formed on the PI surface as the etch mask. The oxide-layer-covered PI surface was then etched using an oxygen-containing plasma to form microroughness and finally, the oxide mask layer was removed using a fluorine-containing plasma. Even though the advantages of this fabrication method for the fine metal lines of flexible electronic devices are apparent, the surface-roughening process consists of numerous steps.

Previously, a single monolayer, polystyrene sphere array, with particles varying in size from tens of nanometers to a few μm, was formed on various substrates with the use of techniques such as spin coating, convective assembly, and tilted-drain, using the polystyrene sphere array as the mask for the etching.[24–26] In this study, as a simple method to form surface roughening on the PI substrate, a polystyrene sphere array that had been coated onto the PI substrate was etched away together with the PI surface using a He/SF_6 plasma, thereby forming a nanoscale surface roughness in one step. After the formation of the nanoscale roughened PI surface, the properties of the surface, in terms of their possible application in silver inkjet printing, were investigated.

2. EXPERIMENTAL DETAILS

For a PI sample, the PI coated with the 120-nm-diameter polystyrene nanosphere array was used. A nanosphere lithography (NSL) method was used to coat the

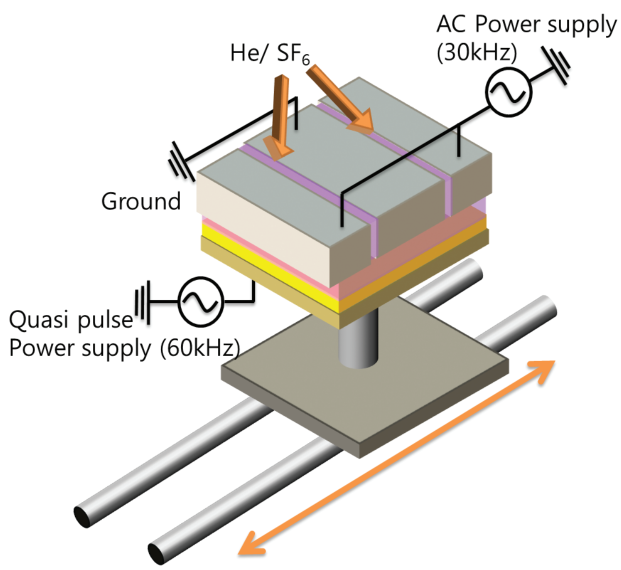

Figure 2. Near-atmospheric-pressure-plasma etching system used in this experiment to roughen the PI surface with the polystyrene nanosphere array using He/SF_6 plasmas. The pressure of the system was maintained at about 500 Torr, which was slightly lower than the atmospheric pressure, for easier and safer control of the gas environment.

polystyrene nanosphere onto the PI surface. The NSL process is a very simple method that does not require any exposure or deposition processes. The NSL allows for the uniform arrangement of a polystyrene nanosphere with particles that vary in size from tens of nanometers to a few μm; furthermore, it can also control the number of layers. The NSL process used in the experiment is shown in Figure 1. First, the 120-nm-diameter polystyrene nanospheres (polystyrene collioid) were sprayed on the deionized water. For self-assembly of the polystyrene nanospheres, an adequate amount of surfactant was dropped on the deionized water. Depending on the amount of surfactant added, a monolayer or multi-layer polystyrene array was formed on the surface of the deionized water. Finally, the PI film picked up the polystyrene nanospheres and the polystyrene-nanosphere-array-covered PI film was dried in preparation for its use as the mask for surface roughening.

The surface roughening of the PI film covered with the polystyrene nanosphere array was carried out using an etching system with near-atmospheric-pressure plasma that was operated at about 500 Torr, which was slightly lower than the atmospheric pressure, to control the purity of the gas environment. The plasma etching system used in the experiment, shown in Figure 2, was composed of 350–400 μm-thick, Al_2O_3-covered aluminum electrodes (three upper electrodes and one lower electrode). With the center electrode grounded, 30 kHz of AC power was applied to the two side electrodes and 60 kHz of AC power was separately applied to the bottom electrode to form more-stable and higher-density plasmas. A reactive gas mixture composed of He and SF_6 was fed to the slits located between the top electrodes.

The contact angle on the PI surfaces before and after the surface roughening was measured not only with water but also with a conductive silver ink. The silver ink (Amogreentech B-30) was composed of 20-nm-diameter silver particles dissolved in an organic solvent. The ink density, viscosity, and surface tension were 1.3 g/cm^3, 16.3 cP, and 32.3 dyne/cm, respectively. To test the adhesion, the silver ink was spin coated on the PI surface for 30 sec at

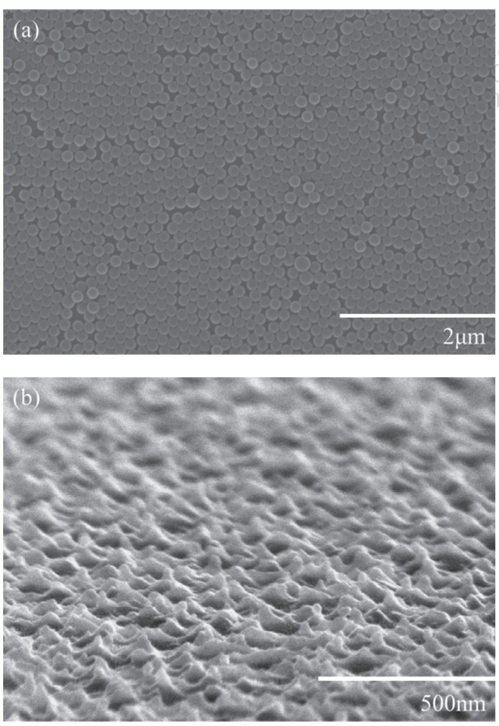

Figure 3. Scanning electron microscope (SEM) images of (a) the PI surface after the coating with the polystyrene nanosphere array and (b) the PI surface after the etching of the PI surface. The PI surface coated with the polystyrene nanosphere array was etched using the near-atmospheric-pressure plasma while flowing He/SF_6 (5 slm:0.3 slm) for 4 min, and by applying 6 kV (30 kHz)–6 kV (60 kHz) to both the upper electrodes and the bottom electrode.

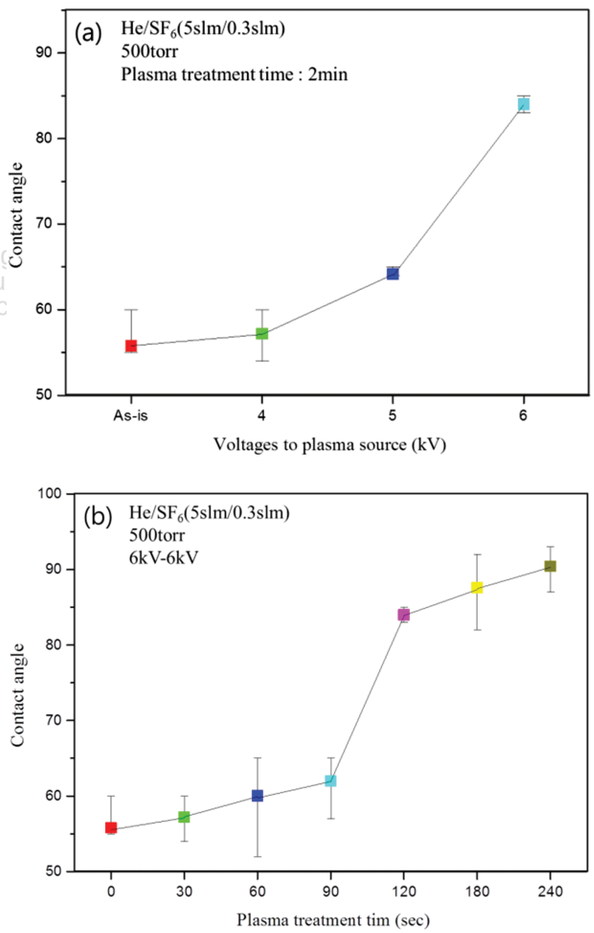

Figure 4. Water contact angles measured on the flat PI surface after the plasma treatment with (a) different AC voltages and (b) different process times. For (a) AC voltages from 4 kV–4 kV to 6 kV–6 kV were applied to the plasma source for 2 min, while flowing He/SF_6 (5 slm:0.3 slm), and for (b) the PI surface was treated with the He/SF_6 (5 slm:0.3 slm) plasma from 0 to 4 min, while applying AC voltages of 6 kV–6 kV to the plasma source.

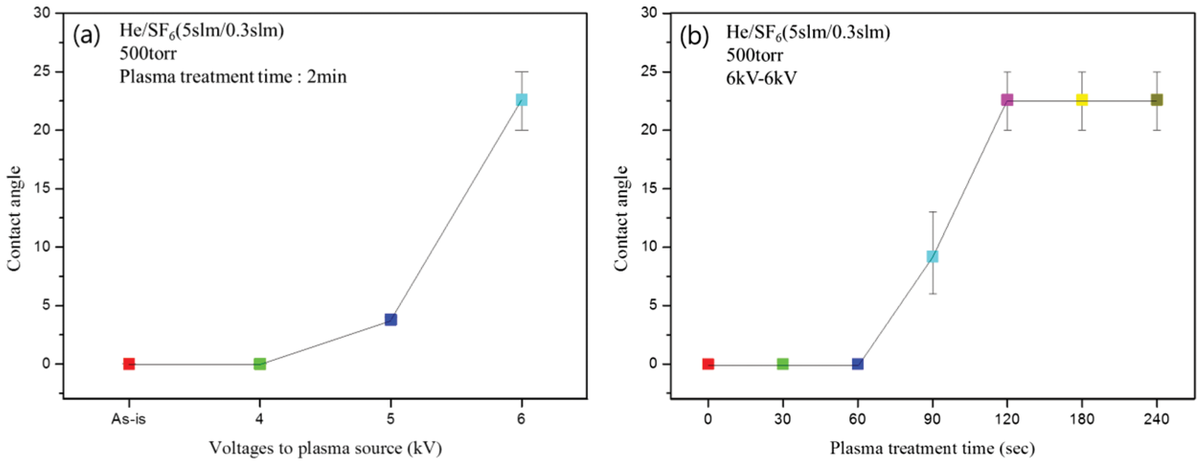

Figure 5. Silver ink contact angles measured on the flat PI surface after the plasma treatment with (a) different AC voltages and (b) different process times. For (a) AC voltages from 4 kV–4 kV to 6 kV–6 kV were applied to the plasma source for 2 min while flowing He/SF_6 (5 slm:0.3 slm), and for (b) the PI surface was treated with the He/SF_6 (5 slm:0.3 slm) plasma from 0 to 4 min while applying AC voltages of 6 kV–6 kV to the plasma source.

2000 rpm, soft baked for 30 min at 150 °C, and finally, hard baked for 1 h at 200 °C. The contact angle was measured with a contact angle analyzer (SEO, Phoenix 450) while tilting the PI substrates at various angles. The surfaces of the PI were observed using a field emission scanning microscope (FE-SEM, Hitachi S-4700).

3. RESULTS AND DISCUSSION

The size of the polystyrene nanospheres controls the peak-to-peak distances of the surface roughness formed after etching. In this study, the polystyrene nanospheres with the 120 nm diameter were used, and Figures 3(a) and (b) show the FE-SEM images of the PI surface after the polystyrene nanosphere-array coating and the PI surface after the etching of the PI surface, respectively. As shown in Figure 3(a), by using the coating method shown in Figure 1, the polystyrene nanospheres were coated relatively uniformly on the PI surface. The PI surface coated with the polystyrene nanosphere array was etched using the near-atmospheric-pressure plasma while flowing He/SF_6 (5 slm:0.3 slm) for 4 min, and by applying 6 kV (30 kHz)–6 kV (60 kHz) to both the upper electrodes and the bottom electrode. As shown in Figure 3(b), after the exposure to the He/SF_6 plasma for 4 min, most of the polystyrene nanospheres were etched away and a textured PI surface with a peak-to-peak distance of about 120 nm and a depth of about 50 nm was exposed. By etching the PI surface coated with the polystyrene nanosphere array, a uniformly-roughened PI surface could therefore be directly obtained without further processing such as a mask-layer removal process. The He/SF_6 plasma used in

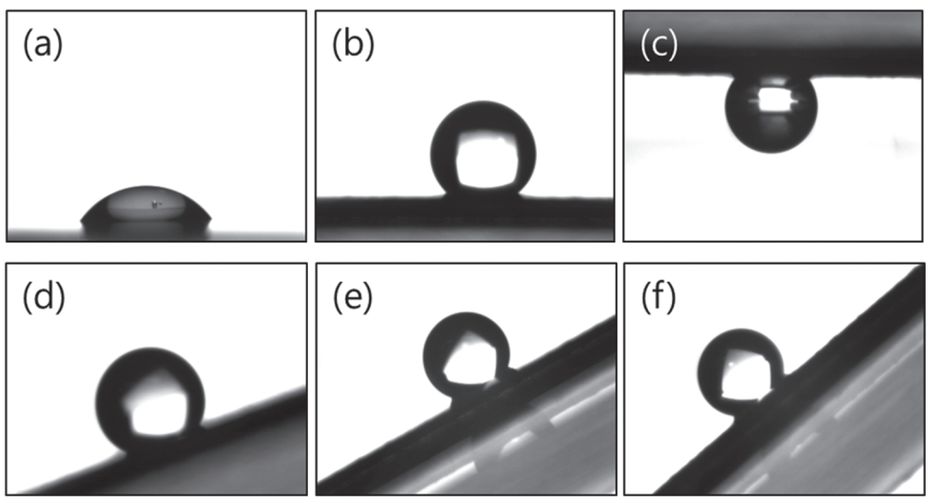

Figure 6. Images of the water contact angles on the plasma-treated PI sample, measured at the different tilting angles of (b) 0°, (c) 180°, (d) 30°, (e) 45°, and (f) 60°. As a reference, the image of the water contact angle on the untreated flat PI surface was included in (a).

Table I. Values of the water contact angles, measured for various PI substrate tilting angles after the surface roughening of the PI surface with the He/SF_6 (5 slm/0.3 slm) plasma at 6 kV–6 kV for 4 min.

Substrate angle (°)	Advancing contact angle (°)	Receding contact angle (°)	Contact angle hysteresis (°)
0	150	150	0
30	135	133	2
45	138	138	0
60	140	136	4
180	140	140	0

Table II. Values of the silver ink contact angles, measured for various PI substrate tilting angles after the surface roughening of the PI surface with the He/SF_6 (5 slm/0.3 slm) plasma at 6 kV–6 kV for 4 min. The silver ink (Amogreentech B-30) was composed of 20-nm-diameter silver particles dissolved in an organic solvent. The ink density, viscosity, and surface tension were 1.3 g/cm^3, 16.3 cP, and 32.3 dyne/cm, respectively.

Substrate angle (°)	Advancing contact angle (°)	Receding contact angle (°)	Contact angle hysteresis (°)
0	30	30	0
30	30	30	0
45	30	26	3
60	27	26	1
180	28	28	0

the experiment not only etched the PI surface but also formed a hydrophobic surface; therefore, by using the He/SF_6 plasma to etch the PI surface, it was possible to obtain both surface roughening and a hydrophobic surface.

The change of the PI surface to a more hydrophobic surface through the He/SF_6 plasma treatment was investigated by treating flat PI samples using the He/SF_6 plasma. Figures 4(a) and (b) show the water contact angles that were measured on the flat PI surface after the plasma treatment with different AC voltages and different process times, respectively. For Figure 4(a), AC voltages from 4 kV–4 kV to 6 kV–6 kV were applied to the plasma source for 2 min while flowing He/SF_6 (5 slm:0.3 slm), and for Figure 4(b), the PI surface was treated with the He/SF_6 (5 slm:0.3 slm) plasma from 0 to 4 min, while AC voltages of 6 kV–6 kV were applied to the plasma source. As shown in the figures, with the increased application of AC voltage to the plasma source, the water contact angle on the plasma-treated flat PI surface was increased from 55° to about 84°. As shown in Figure 4(b), the increase of the plasma treatment time increased the contact angle; however, when the plasma treatment time was higher than 2 min at 6 kV–6 kV, the contact angle was almost saturated and about 90° of the contact angle could be obtained at 4 min for the flat PI surface.

Using the silver ink described in the "Experimental" section, the contact angles on the plasma-treated flat PI surface were also measured under the plasma treatment conditions in Figure 4, and the results are shown in Figures 5(a) and (b) for different AC voltages and different plasma treatment times, respectively. Silver ink typically has a lower surface tension (<30 mN/m) compared with water (>70 mN/m) due to an organic solvent used in the ink. As shown in the figures, the contact angle of the silver ink on the flat PI surface without the plasma treatment was therefore ~0° and, even though the contact angle was increased with the increased application of AC voltage to the plasma source, the highest contact angle at 6 kV–6 kV of AC voltages was about 22° and no further increase of the contact angle was observed after 2 min.

The contact angles were also measured after the plasma treatment under the conditions shown in Figure 3(b). Figures 6(b)–(f) show the water contact angles on the plasma-treated PI sample measured at different tilting angles from 0° to 180°. As a reference, an image of the water contact angle on the untreated flat PI surface was also included as Figure 6(a). The measured values of the water contact angles are also shown in Table I.

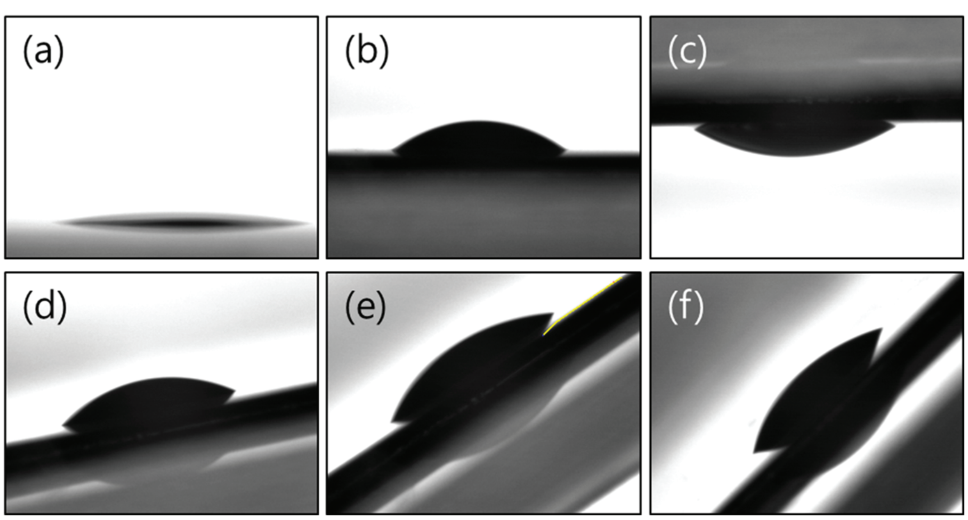

Figure 7. Images of the silver ink contact angles on the plasma-treated PI sample, measured at the different tilting angles of (b) 0°, (c) 180°, (d) 30°, (e) 45°, and (f) 60°. As a reference, the image of the silver ink contact angle on the untreated flat PI surface was included in (a).

As shown in Figure 6 and Table I, after the surface roughening of the PI surface with the He/SF_6 (5 slm/0.3 slm) plasma at 6 kV–6 kV for 4 min, the water contact angle was increased from about 90° to 150°, and an improved hydrophobic surface property was therefore observed after the surface roughening. In addition, when the PI sample was tilted, the water droplet did not roll off the PI surface in accordance with the lotus effect,[27, 28] and the difference between the advancing contact angle and the receding contact angle was close to 0°, indicating that the water droplet was in full contact with the PI surface.

The silver ink contact angles were also measured on the PI surface after the plasma treatment. Figures 7(b)–(f) show the silver ink contact angles on the plasma-treated PI sample measured at different tilting angles. The silver ink contact angle on the untreated flat PI surface is shown in Figure 7(a) as a reference. The silver contact angle values are also shown in Table II. As shown in Figure 7 and Table II, after the surface roughening of the PI surface under the same conditions in Figure 6, the silver ink contact angle was also increased from 22° to 30°, similar to the water contact angle in Figure 6, indicating that it may be possible to decrease the silver ink linewidth in a more controlled manner. The hysteresis angle was also very low, indicating that the adhesion of the silver ink to the PI surface might have been improved after the roughening.

The adhesive property between the silver ink and the PI surface before and after the surface roughening was investigated by a cross-cut tape test (ASTM D3359B). The PI sample coated with the polystyrene nanosphere array was etched under the conditions in Figure 6 and, as a reference, the flat PI sample was also was treated under the same conditions. The silver ink was spin coated on both the surface-roughened and flat PI samples and, after the sintering, the adhesive property was measured with the tape test and the results are shown in Figure 8. As shown in Figure 8, for the flat PI surface, most of the silver layer was peeled off by the tape testing while, for the surface-roughened PI surface, no peeling of the silver layer was observed, indicating an improved adhesive property after the surface roughening that was possibly due to the increased contact area between the silver ink and the PI surface. It is therefore believed that, after a He/SF_6 plasma etching of a PI surface coated with a polystyrene nanosphere array, as presented in this study, it is possible to enhance both linewidth control and adhesion.

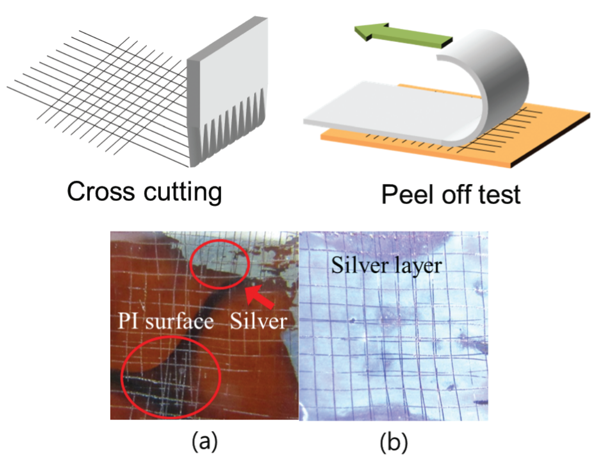

Figure 8. The adhesive property measured between the silver ink and the PI surface before and after the surface roughening using a cross-cut tape test (ASTM D3359B). The PI sample coated with the polystyrene nanosphere array was etched under the conditions in Figure 6 and, as a reference, the flat PI sample was also treated under the same conditions. The silver ink was spin coated on both the surface-roughened and flat PI samples and, after the sintering, the adhesive properties were measured with the tape testing.

4. CONCLUSIONS

In this study, to roughen the PI surface more easily, a PI surface masked with a 120-nm-diameter polystyrene nanosphere array was formed using the NSL technique, and both the polystyrene nanospheres and the PI surface were etched together using a He/SF_6 plasma. By etching the PI surface masked with the polystyrene nanospheres, a nanoscale surface roughness measuring 120 nm wide and 50 nm deep could be easily formed in one step. In addition, a hydrophobic surface was obtained through the etching of the PI surface with SF_6 gas. Compared to the flat PI sample treated with the same plasma, the surface-roughened PI sample exhibited an improvement of the silver ink contact angle from 22° to 30°, indicating the improved fine-linewidth control of the silver inkjet line; the silver ink's adhesive property was also improved by increasing the contact area between the silver ink and the PI surface. It is believed that the surface-roughening method used in this study can be applied to improve both linewidth and the adhesion of inkjetted materials to the flexible substrates that are required for next-generation flexible electronics.

Acknowledgments: This work was carried out through a project supported by Samsung Electro-Mechanics to improve adhesive force using modified atmospheric-pressure plasma (S-2014-1507-0011).

References and Notes

1. L. An, Y. Zheng, K. Li, P. Luo, and Y. Wu, *Journal of Vacuum Science & Technology B: Microelectronics and Nanometer Structures* 23, 4 (**2005**).
2. R. Blossey, *Nat. Mater.* 2, 5 (**2003**).
3. L. Boinovich, A. M. Emelyanenko, V. V. Korolev, and A. S. Pashinin, *Langmuir* 30, 6 (**2014**).
4. Y. L. Loo, T. Someya, K. W. Baldwin, Z. Bao, P. Ho, A. Dodabalapur, H. E. Katz, and J. A. Rogers, *Proc. Natl. Acad. Sci. USA*. 99, 16 (**2002**).
5. J. Zaumseil, T. Someya, Z. Bao, Y. Loo, R. Cirelli, and J. A. Rogers, *Appl. Phys. Lett.* 82, 5 (**2003**).
6. S. H. Ko, I. Park, H. Pan, C. P. Grigoropoulos, A. P. Pisano, C. K. Luscombe, and J. M. Fréchet, *Nano Lett.* 7, 7 (**2007**).

7. F. Garnier, R. Hajlaoui, A. Yassar, and P. Srivastava, *Science* 265, 5179 (**1994**).
8. J. Chung, N. Bieri, S. Ko, C. Grigoropoulos, and D. Poulikakos, *Appl. Phys. A* 79, 4 (**2004**).
9. J. Wang, Z. Zheng, H. Li, W. Huck, and H. Sirringhaus, *Nat. Mater.* 3, 3 (**2004**).
10. S. E. Burns, P. Cain, J. Mills, J. Wang, and H. Sirringhaus, *MRS Bull* 28, 11 (**2003**).
11. S. H. Ko, H. Pan, C. P. Grigoropoulos, C. K. Luscombe, J. M. Fréchet, and D. Poulikakos, *Appl. Phys. Lett.* 90, 14 (**2007**).
12. X. Dai, X. Huang, F. Yang, X. Li, J. Sightler, Y. Yang, and C. Li, *Appl. Phys. Lett.* 102, 16 (**2013**).
13. X. Dai, X. Huang, F. Yang, X. Li, J. Sightler, Y. Yang, and C. Li, *Appl. Phys. Lett.* 102, 16 (**2013**).
14. H. Gan, X. Shan, T. Eriksson, B. Lok, and Y. Lam, *J. Micromech. Microeng.* 19, 5 (**2009**).
15. A. Garcia, J. Polesel-Maris, P. Viel, S. Palacin, and T. Berthelot, *Adv. Funct. Mater.* 21, 11 (**2011**).
16. R. J. Good, *J. Am. Chem. Soc.* 74, 20 (**1952**).
17. Z. Guo and W. Liu, *Appl. Phys. Lett.* 90, 22 (**2007**).
18. J. Han, B. Kim, J. Li, and M. Meyyappan, *Appl. Phys. Lett.* 102, 5 (**2013**).
19. G. Jeong, J. Park, K. Lee, J. Jang, C. Lee, H. Kang, C. Yang, and S. Suh, *Microelectron. Eng.* 87, 1 (**2010**).
20. D. Liaw, K. Wang, Y. Huang, K. Lee, J. Lai, and C. Ha, *Prog. Polym. Sci.* 37, 7 (**2012**).
21. M. Matsumoto, Y. Inayoshi, M. Suemitsu, T. Yara, S. Nakajima, T. Uehara, and Y. Toyoshima, *Thin Solid Films* 516, 19 (**2008**).
22. A. D. Ormonde, E. C. Hicks, J. Castillo, and R. P. Van Duyne, *Langmuir* 20, 16 (**2004**).
23. J. B. Park, J. Y. Choi, S. H. Lee, Y. S. Song, and G. Y. Yeom, *Soft Matter* 8, 18 (**2012**).
24. S. Seo, C. G. Choi, Y. H. Hwang, and B. Bae, *J. Phys. D* 42, 3 (**2009**).
25. A. Shimoni, S. Azoubel, and S. Magdassi, *Nanoscale* 6, 19 (**2014**).
26. Q. Yu, Z. Zeng, W. Zhao, H. Li, X. Wu, and Q. Xue, *Chem. Commun.* 49, 24 (**2013**).
27. D. Zang, F. Li, X. Geng, K. Lin, and P. S. Clegg, *The European Physical Journal E* 36, 6 (**2013**).

Received: 16 August 2014. Accepted: 5 March 2015.